Dalton Transactions

PERSPECTIVE

Cite this: *Dalton Trans.*, 2019, **48**, 5476

On the preferences of five-membered chelate rings in coordination chemistry: insights from the Cambridge Structural Database and theoretical calculations†

Maryam Bazargan,[a] Masoud Mirzaei, *[a] Antonio Franconetti [b] and Antonio Frontera *[b]

Received 4th February 2019,
Accepted 20th March 2019

DOI: 10.1039/c9dt00542k

rsc.li/dalton

The purpose of this review is to give an overview of three important *N*-bidentate ligands: 1,10-phenanthroline (phen), 2,2′-bipyridine (bpy), and ethylenediamine (en). We have not attempted to be comprehensive because of the huge amount of activity being done in coordination chemistry using these ligands. Instead we present a full structural and geometrical study by using the Cambridge Structural Database (CSD) combined with theoretical calculations that allow us to parameterize their coordinating properties and ability to coordinate to transition and non-transition metals. More importantly, we illustrate that upon coordination and formation of the five-membered chelate ring, these ligands are able to adapt themselves to the requirements of the different metals by changing the MN distances and NMN angles. Therefore, a redefinition of the preferences of these ligands to metals with large ionic radii is needed. Finally, we will present some facts about the participation of these ligands in inorganic–organic hybrids (IOHs) based on Keggin polyoxometalates (POMs).

1. Introduction

Nowadays, one of the main purposes of modern chemistry and crystal engineering is the design and creation of new crystalline materials with tailored properties. To understand the mysteries of crystal engineering, a deep comprehension of non-covalent interactions and the effects of their intricate combinations is needed. Therefore, it is necessary to find the logical relationship between the molecular shape, symmetry and the nature of intermolecular forces, such as hydrogen bonds, π···π stacking, CH···π, lone pair···π interactions, *etc.*[1–4] The study and comprehension of the geometrical behavior of ligands and their coordination properties to metal centers are also important to succeed in crystal engineering. However, the inability to completely synthesize desired crystals seems to be a great limitation in this field. Undoubtedly, ligand design can be an important issue for crystal designers because of its significant role in the complex stability and metal ion selectivity. Ligand design involves the examination of existing metal–ligand complex structures according to the available experimental geometrical data and also computer models. The use of innovative arrays of donor atoms, that are chosen to bind to one or more metal ions, allows creating complexes that display new properties.[5–7] Therefore, developing, designing and investigating highly organized ligands have a bright future since they are capable of binding substrates with high efficiency and selectivity. Accordingly, two main steps in the ligand design strategy arise: (i) full understanding of the structural information of the organic ligands such as the rigidity and flexibility of the skeleton, the nature of the donor atoms, chelating ring size and coordination behavior;[8] (ii) studying of the possible participation of the ligand in non-covalent intermolecular interactions *via* the ligand backbone or its functional groups that link directly to supramolecular chemistry.[9]

The aim of this review is to provide the crystal engineering community with a thorough structural study of three amine and/or imine ligands; ethylenediamine (en), 2,2′-bipyridine (bpy), and 1,10-phenanthroline (phen). This is achieved by examining the Cambridge Structural Database (CSD) and performing theoretical calculations of their coordination behavior with different metal centers. We begin with a brief presentation of the foundation of rigidity *vs.* flexibility of N-donor ligands and continue with more specific research on the *N*-bidentate ligands (phen/bpy/en) as selected examples of preorganized and non-preorganized ligands. The full CSD results help us to

[a]*Department of Chemistry, Faculty of Science, Ferdowsi University of Mashhad, 917751436 Mashhad, Iran. E-mail: mirzaeesh@um.ac.ir, mirzaei487@yahoo.com*
[b]*Departament de Química, Universitat de les Illes Balears, Crta. de Valldemossa km 7.5, Palma de Mallorca, Baleares E-07122, Spain. E-mail: toni.frontera@uib.es*
†Electronic supplementary information (ESI) available. See DOI: 10.1039/c9dt00542k

realize that these ligands are versatile since they are able to bind with a variety of metal centers. We relate this feature to the formation of five-membered chelate rings, which is favorable in a variety of metals with quite different ionic radii and electronic configurations. Finally, their inorganic–organic hybrids (IOHs) based on Keggin polyoxometalates (POMs) will be presented. This review will inspire more interest in the development of new materials with more predictable properties.

2. Rigid *vs.* flexible N-donor ligands

Many different factors affect the final solid state structure in the crystals of coordination compounds, such as the coordination geometry of the central metal ion, binding modes of the organic ligands, and the synthesis conditions.[8,10] To adequately select a ligand, it is important to know its geometrical characteristics and behavior. A library of compounds and their key features is convenient for a better design of the target structure. Many articles and CSD searches have showed that many structures are composed of neutral flexible and/or rigid N-donor ligands (see Fig. 1).[11,12] However, the lack of negative charge in these ligands may cause synthetic troubles because the anionic counterpart needs to be incorporated into the framework for neutrality. It is well known that flexible N-donor ligands have conformational freedom resulting from their rotation around the single bond(s). They can chelate the metal ion through their ends or act as linkers bridging the metal centers and increasing the dimensionality of the system. Accordingly, more flexibility always leads to lower selectivity. Also, some investigations have shown that the long alkyl chain in the flexible N-donor ligands can be suitable for the construction of chiral frameworks.[13] Nonetheless, rigid N-donor ligands have only limited movement in their backbone because of their planarity and stability which arise from their aromaticity. Moreover, the reaction of the rigid ligands is comparatively easy to control and reduce the uncertainty of the assembly during the formation of the final product. The use of rigid N-donor ligands prevents the formation of high dimensional frameworks and they are also known as "terminators".[14] Finally, rigid N-donor ligands have more predictable behaviors, due to their restrictive coordination modes and they are good candidates for use in crystal engineering.

3. *N*-Bidentate ligands

In this section, three commonly used *N*-bidentate ligands (phen, bpy and en) are introduced briefly. They are versatile ligands for designing and synthesizing metal organic complexes (MOCs) with desired properties in molecular biology, such as DNA cleavage or insertion reagents,[15–17] contrast agents for magnetic resonance imaging,[18,19] chelation therapies[20] and metalloenzymes.[21] Several reviews have been published summarizing their properties.[22,23] In the chemistry of nitrogen donor ligands, en has been very popular since the naissance of coordination chemistry.[24] The bpy ligand was discovered at the end of the nineteenth century and has gained renewed interest due to its importance in fields like photovoltaics,[25,26] OLEDs[27,28] and molecular sensors.[29,30] Finally, phen

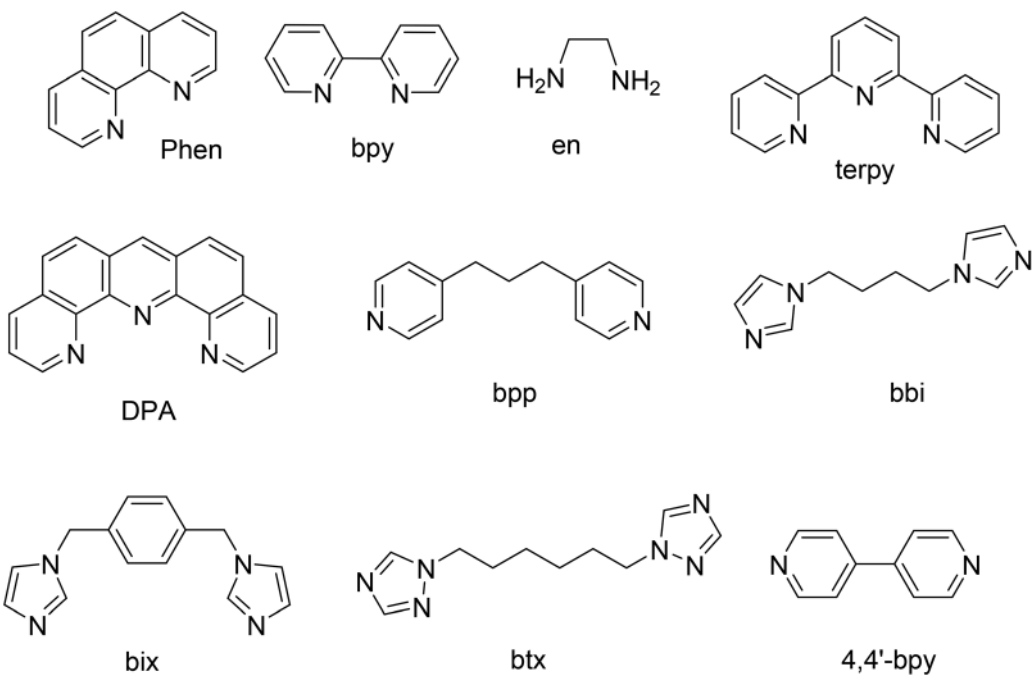

Fig. 1 Chemical representation of rigid and flexible N-donor ligands. Phen: 1,10-phenanthroline; bpy: 2,2′-bipyridine; en: ethylenediamine; terpy: terpyridine; DPA: dipyridoacridine; bpp: 1,3-di(4-pyridyl)propane; bbi: 1,1′-(1,4-butanediyl)bis(imidazole); bix: 1,4-bis(imidazol-1-ylmethyl)benzene; btx: 1,1′-(1,6-hexanediyl)bis(1*H*-1,2,4-triazole); 4,4′ bpy = 4,4′-bipyridine.

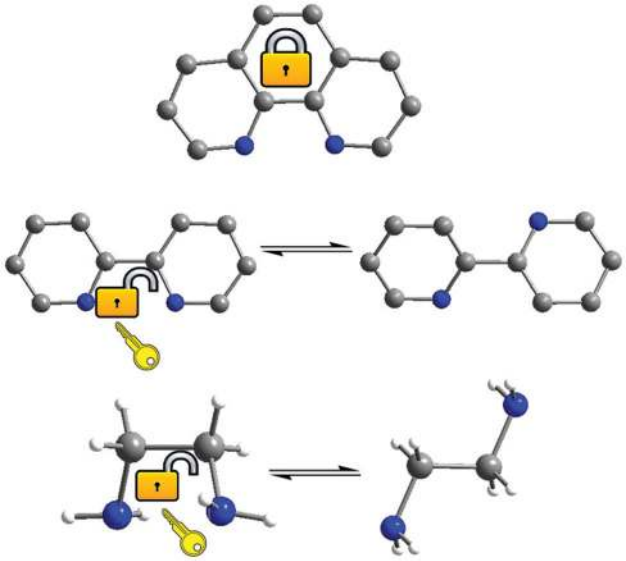

Fig. 2 Representation of the *cis*-locked mode in the rigid phen ligand (top) and the C–C bond rotation in the bpy/en ligand (down).

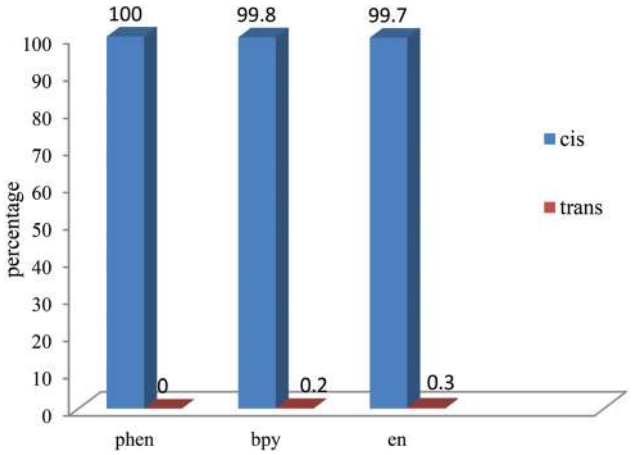

Scheme 1 *cis- versus trans*-mode in the phen/bpy/en complexes.

is known as a rigid coplanar ligand that is important in fields like genetic engineering and molecular biology due to its efficiency to cleave the DNA and RNA backbone.[15,16,31] Also, the electron-conjugated heteroaromatic system in phen/bpy rigid ligands makes them adequate to establish π–π inter-ligand interactions and create supramolecular architectures with interesting photoluminescence, electrochemical,[32–34] magnetic[35] and antiproliferative[36] applications. Their empty π* orbitals have good potential to accept electrons from metal centers and, consequently, some of their MOCs have an intense metal-to-ligand charge-transfer (MLCT), which is characteristic in the visible region of spectra. Therefore, they can be good candidates for optical and photoelectronic materials.[37–39] The sp^3-hybridzed N-donors of en present higher basicity than sp^2-hybridized pyridyl N-donors and the influence on their metal complexes will be further discussed below. Regarding the C–C bond rotation, bpy and en ligands present *cis*/*trans* isomerism, whereas the phen ligand is pre-organized in the *cis*-locked conformation (Fig. 2).

4. Preorganized ligands

The earliest investigations of preorganized ligands involved basically multidentate macrocyclic molecules such as crown ethers, cryptands and aza-macrocycles. In 1988 Cram stated that "preorganization is a central determinant of binding power".[40] Since this discovery, a large amount of research studies focused on this family of ligands in order to successfully design and construct new crystalline materials with tailored applications like sensors, catalysts and magnetic resonance imaging agents.[41–43] Hemoglobin and vitamin B12 are also well-known biological metallocomplexes based on pre-organized macrocyclic ligands. The main synthetic disadvantage of macrocyclic ligands is the final cyclization step that is usually difficult with relatively high-cost and low yield. Thus, the use of non-macrocyclic preorganized ligands is convenient to overcome this problem. Although these ligands do not have a cavity, the arrays of donor atoms show suitable selectivity for metal ions by creating chelate rings. Herein, the ability to form chelate rings of phen/bpy/en is examined. A CSD survey revealed that the *cis*-form is dominated even for the non-pre-organized en ligand (see Scheme 1) which is attributed to the chelate effect. Therefore, their structures will be highly predictable since it prefers chelate coordination instead of the bridge form (see Fig. 2). From the view point of crystal engineering, pre-organized ligands act as structural directing tools, which is the case of the three ligands studied herein. That is, based on the CSD analysis given in Scheme 1, bpy and en, which are not pre-organized ligands from a classical point of view, have a high preference to form chelate rings (*cis* conformation >99.7%) and, consequently, they act as if they were preorganized ligands.[44,45]

5. Datasets and methods

Crystallographic data were retrieved from the CSD version 5.38 (update May 2017) using ConQuest, version 1.19. The structure searches were restricted to the phen, bpy and en ligands without any restriction regarding the coordinated metal (M). N–M distances and N–M–N angles were determined for all structures by using ConQuest and analyzed using Mercury version 3.9. The results are limited to mononuclear complexes (compounds with one type of metal and not mix metals).

6. CSD structural study of the phen/bpy/en complexes

6.1. Geometrical preference

As shown in Scheme 2 the majority of phen/bpy/en ligands are mononuclear due to their preference for the chelate coordi-

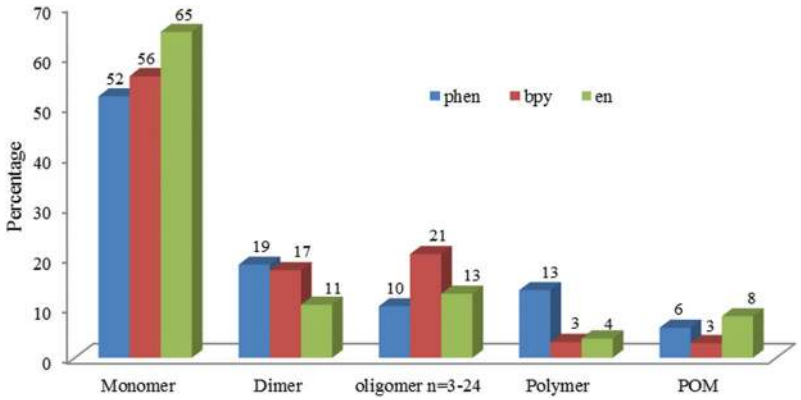

Scheme 2 Structural preferences for phen, bpy and en in the mononuclear complexes that are extracted from the CSD data.

nation mode. However, dinuclear, polynuclear (n = 3–24) and polymeric compounds have also been prepared by using auxiliary ligands such as aromatic or aliphatic carboxylic acids or flexible multidentate N-donor ligands. The purpose of using a mixture of ligands is to enhance some properties in the final structure. For example, coordination complexes of [Ln(β-diketonate)$_3$phen] (Ln = Eu^{3+} and Tb^{3+}) showed great luminescence properties specially in solar cells.[46] It is worth mentioning that in the absence of phen, β-diketonate complexes generally form hydrated complexes like [Ln(β-diketonate)$_3$(H_2O)$_2$], where the water molecules quench the luminescence.

It is well known that $[M(phen/bpy/en)_3]^{n+}$ complexes are chiral and form right and left handed enantiomers (Δ or Λ). However, both the Δ and Λ configurations usually co-exist in the crystals, resulting in racemic compounds. To date, only a limited number of crystals with one enantiomer have been reported.[47–50]

6.1.1. 1,10-Phenanthroline (phen). Although the chelating bidentate mode is predominating for phen (Fig. 3, **I**a), in a very unusual structure phen can act as a monodentate ligand (Fig. 3, **I**d) such as [PtCl(phen)(PEt_3)$_2$][BF_4] and [PdCl(phen)(PPh_3)$_2$][BF_4]·(CH_3)$_2$CO. Their X-ray diffraction data revealed that both M–N and M–N′ bond distances are unequal (2.13 and 2.84 Å for M = Pt; and 2.09 Å and 2.68 Å for M = Pd).[46,51] The elongation of the Pd/Pt–N′ bonds (0.34–0.18 Å) is significantly longer than the sum of the ionic radii (2.50 Å). It is

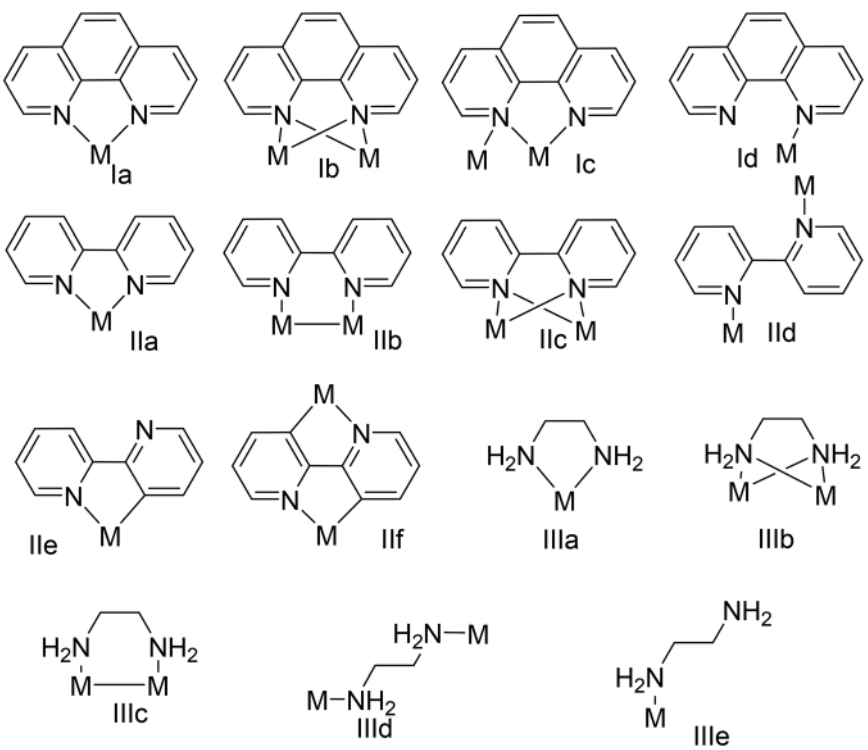

Fig. 3 Classification of coordination modes found for the phen, bpy and en ligands based on the CSD analysis.

attributed to the known preference of Pt(II) and Pd(II) for a square planar geometry, along with steric effects that prevent the formation of the $[MCl(phen)(PR_3)_2]^+$ cation. In a few complexes of Na, K and Rb, phen acts as both a chelate and a bridging ligand simultaneously.[52–56] This rare phenomenon can be attributed to the large size of alkaline group elements as well as π-stacking and crystal packing effects (Fig. 3, **I**b and **I**c). As shown in Scheme 3 (blue columns), the probability of 1 : 4 and 1 : 5 metal to ligand ratios is negligible. In fact, the 1 : 4 ratio is only observed for Ca, Ba and Pb metal centers and the 1 : 5 ratio only occurs for Ba. All of these metal ions have ionic radii larger than 1.1 Å. It is worth commenting how four or five bulky ligands are able to arrange around these metal centers: $[Ca(phen)_4]I_2$ (**1**),[57] $[BrBa(phen)_4]Br{\cdot}MeOH$ (**2**), $[Ca(phen)_4](ClO_4)_2{\cdot}2L$ L = (4-(dimethylamino)benzaldehyde molecule) (**3**),[58] $[Pb(phen)_4](ClO_4)_2$ (**4**), $[ClO_4Pb(phen)_4]$ (**5**)[59] and $[Ba(phen)_5]{\cdot}MeCN$ (**6**),[57] (**1** and **6** are shown in Fig. 4). The metal is an eight-coordinated distorted square antiprism in compounds **1**, **3** and **4**, a nine-coordinated distorted monocapped square antiprism in complexes **2** and **5** and a ten-coordinated distorted bicapped square antiprism in compound **6**. Consequently, for reducing the steric hindrance in these complexes, the metal center moved outside the ligand planes or two pairs of ligands lied in the quasi-parallel planes.

6.1.2. 2,2′-Bipyridine (bpy). As mentioned before, *cis*- and *trans*-conformations are possible for bpy (Fig. 2, middle).

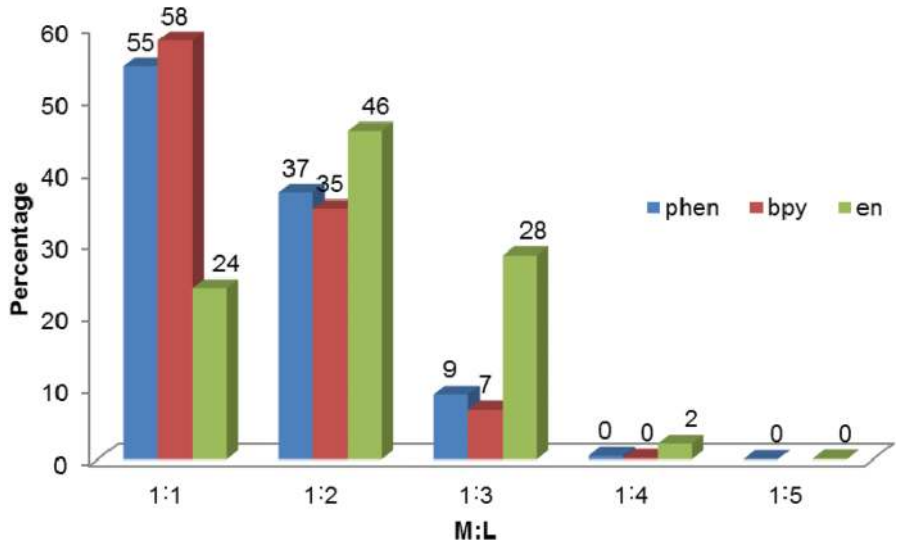

Scheme 3 Percentage of the metal to ligand ratio in the mononuclear monomeric compounds.

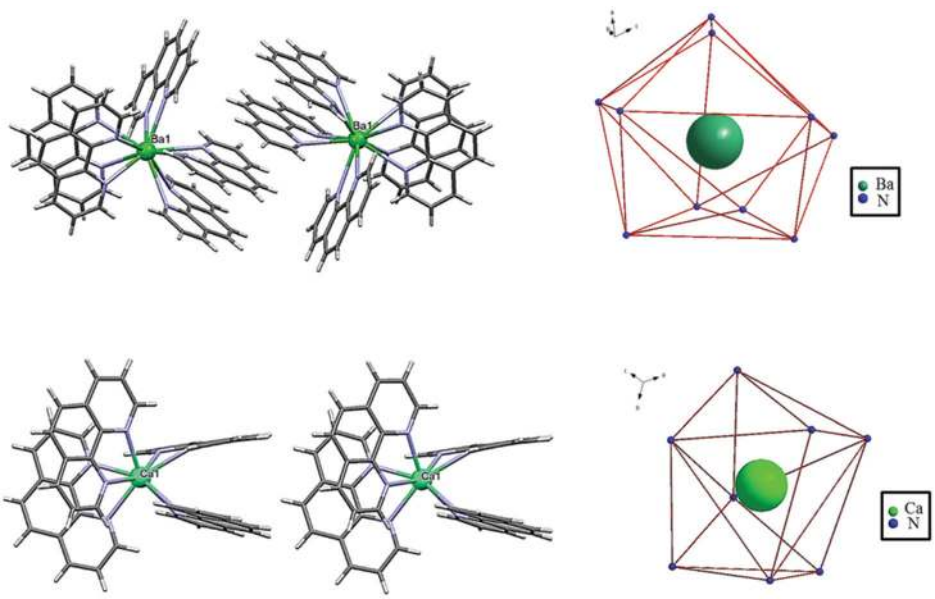

Fig. 4 Geometrical preference for the $Ca(phen)_4$ (**1**) and $Ba(phen)_5$ (**6**). Figure reproduced from ref. 57 and 58.

These two conformers are different in several aspects such as dipole moment and charge distribution. Theoretical calculations and solid state and solution studies have shown that the most stable one is the *trans*-form. Destabilization of the *cis*-conformer is caused by steric repulsion of two hydrogen atoms (H3,H3′) and coulombic repulsion of the nitrogen lone pairs.[60] In spite of these facts, as shown in Scheme 1, the *cis*-conformation is commonly found in bpy complexes because of the formation of a five-membered chelate ring (Fig. 3, **II**a). Other coordination modes such as **II**b (chelating and bridging), **II**c (dinucleating), **II**d (bridging), **II**e, **II**f and **II**g (*N*′, C(3) bonded tautomeric form) are rare or extremely rare. For the latter, the *trans*-conformation in combination with an appropriate metal intermediate may activate the C(3)–H bond of one pyridine ring, forming an *N*′, C(3) five-membered cyclometalated ring.[61] This process is known as rollover cyclometalation and is feasible for all ligands that can adopt at least the bidentate coordination mode and that are flexible enough to undergo internal rotation such as bpy and 2-(2-thienyl)pyridine. The reaction must involve, after chelation, partial decomplexation of the ligand that undergoes internal rotation around a suitable bond and promote the selective activation of a C–H bond and the formation of the metallocycle. As shown in Scheme 3 (red columns), the probability of forming complexes with metal to ligand ratios of 1 : 3 and 1 : 4 is low and there is not any example in the literature with a 1 : 5 ratio. For the very rare 1 : 4 ratio, all complexes have the $[M(bpy)_4]^{n+}$ formula, where M = Pb, Sm, Eu, Yb, Lu and U in which the bpy ligands establish π-stacking interactions in the solid state.[62–64]

6.1.3. Ethylenediamine (en). The behavior of the en ligand is very similar to that of phen/bpy ligands. Therefore, despite its flexible backbone, the *cis*-form (chelating bidentate mode) is dominant. However, monodentate (**III**e), bridging (**III**b and **III**d) and dinucleating (**III**c) fashions also exist (Fig. 3). Metal to ligand ratios of 1 : 4 and 1 : 5 (see Scheme 3) are relatively rare. Indeed, the 1 : 4 ratio is observed for one transition metal Y, three group 2 elements Ca, Sr, and Ba and lanthanoids (Lns) like La, Ce, Pr, Nd, Sm, Eu, Gd, Dy, Ho, Er, Tm and Yb. The 1 : 5 ratio is only observed for $[La(en)_5]Cl_3{\cdot}en{\cdot}CH_2Cl_2$ in a distorted bicapped square antiprism coordination geometry around the La^{3+}.[65]

6.2. Metal preference

Neutral *N*,*N*′-coordinated phen/bpy/en ligands are able to form stable complexes with most of the metal centers in a variety of oxidation states. Most of their mononuclear complexes involve d block elements followed by f block elements (see Scheme 4). As expected due to their large ionic size and small electronegativity, the coordination compounds of the alkali and alkaline earth metals are relatively rare. The frequencies of the phen/bpy/en complexes are shown in Fig. S1.† It clearly reveals that these ligands can fit themselves to various types of metal ions simply by moving the metal center with respect to the ligand plane (shortening or lengthening of the M–N coordination bonds) and leading to some distortion of the metal/nitrogen/carbon angle (see Table 1). As the metal ion radius increases, the number of compounds decreases in the following order phen > bpy > en. This is due to several reasons: (i) The phen ligand is rigid with an entropically favored chelate binding (*cis* conformation) compared to en and bpy; (ii) low-lying LUMO orbitals in the phen enhance the π-back acceptance compared to the other two ligands;[20,66] (iii) the experimental data revealed that the stability constant data (log *K*) for many complexes are in the phen > bpy > en order.[67,68]

7. Five-membered chelate ring

Many articles and reviews reported that the important factor for metal ion selection is the chelate ring size in which five-membered chelate rings promote selectivity for large metal ions with an ionic radius (r^+) close to 1.0 Å. Theoretical calcu-

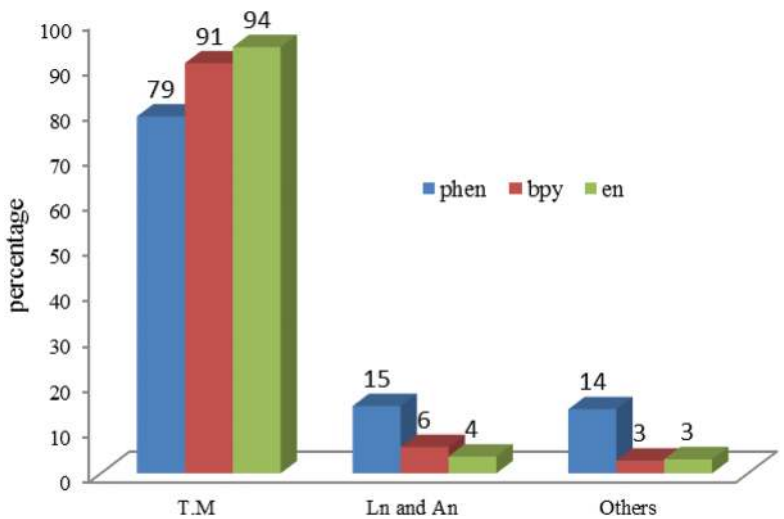

Scheme 4 Percentage of the metal centers in the MOCs of phen/bpy/en, which is extracted from the CSD data.

Table 1 Details of the five-membered chelate ring geometry for the 3d, 4d, 5d, 4f and all compounds by phen/bpy/en up to now, which are extracted from the Cambridge Structural Database (version 5.38, updated May 2017). Note: Ang. 1–4 are shown on the Fig. 5 right

Compounds	Number of compounds	*r* (M–N) average (Å)	*d* (N–N) average (Å)	*α* (N–M–N) average (°)	Ang. 1 average (°)	Ang. 2 average (°)	Ang. 3 average (°)	Ang. 4 average (°)
phen								
3d	6857	2.097	2.667	79.109	113.224	117.040	117.040	113.59
4d	2003	2.225	2.694	74.881	114.602	117.527	117.571	114.654
5d	829	2.258	2.681	73.765	115.400	117.262	117.341	115.154
4f	1366	2.609	2.718	62.829	119.656	118.096	118.065	119.680
All	11 909	2.209	2.681	75.559	114.391	117.319	117.322	114.524
bpy								
3d	4469	2.074	2.623	78.600	115.235	115.122	115.071	115.285
4d	2607	2.121	2.634	77.003	115.785	115.333	115.376	115.795
5d	979	2.125	2.627	76.610	116.156	115.267	115.259	116.156
4f	405	2.583	2.687	62.739	121.283	116.253	116.537	121.248
All	8788	2.123	2.631	76.985	115.865	115.273	115.292	115.831
en								
3d	1884	2.036	2.175	83.75	108.910	109.069	109.188	108.848
4d	393	2.115	2.747	81.249	109.129	109.092	109.808	109.162
5d	266	2.124	2.732	80.729	109.908	109.008	109.015	109.990
4f	96	2.594	2.813	65.706	114.331	109.838	109.664	114.464
All	2704	2.077	2.726	82.447	109.187	109.213	109.274	109.126
Ideal five-membered ring[68–70]	—	2.5	2.83	69	120			120

lations show that for five-membered NCCNM chelate rings the ideal size for the N–M distance is 2.5 Å and the N–M–N angle is 69°.[68–70] Here, by using the CSD search, we want to survey this relationship using phen/bpy/en ligands since they have great potential to form five-membered chelate rings. As is shown in Scheme 5 (up), there is an inverse relationship between the bond length and the bond angle. It means that the variation of the NMN angle of the five-membered chelate rings is directly related to the MN bond length. Therefore, by increasing the metal ion size, the N–M–N angle becomes smaller and its corresponding M–N bond becomes longer (see Fig. 5 left and Table 1). This relationship and flexibility between the bond length and angle cause the ligand cavity NCCN matching itself with most of the elements. The NN distances for phen/bpy/en compounds are very similar, see Scheme 5 (down) and by increasing the metal ion size the

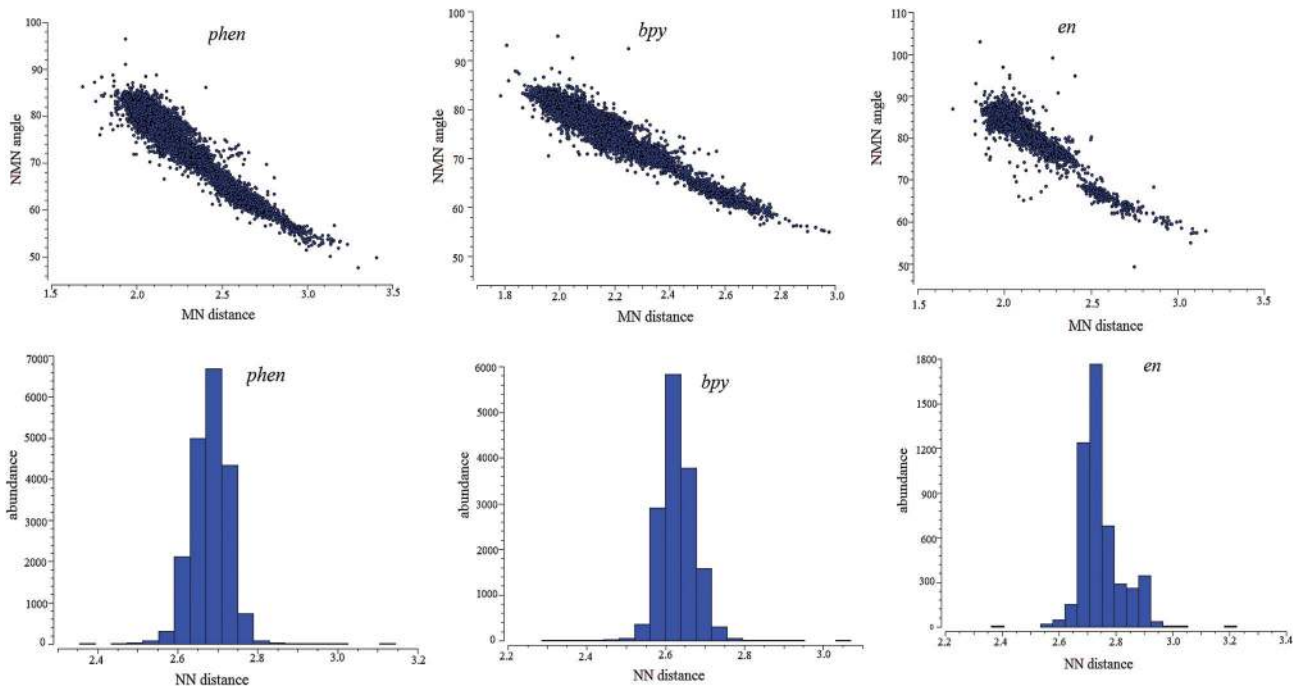

Scheme 5 Up: Inverse relationship between the MN bond length and the NMN bond angle in the phen/bpy/en complexes. Down: Distribution of the NN distance for phen/bpy/en ligands in their compounds.

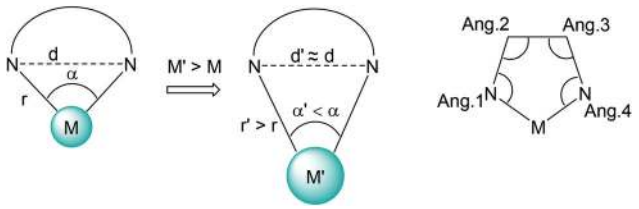

Fig. 5 Left: Metal ion size and its effect on the bond length and bond angle in the five-membered chelate ring. Right: Angle labelling for Table 1.

M–N coordination distances lengthen and, concomitantly, the values of Ang. 1, Ang. 4 and the N···N distance increase.

Table 1 lists the structural details and CSD reference codes of all the five-membered chelate rings created by phen/bpy/en ligands (see Fig. 5 right). Some important issues arise from the inspection of the results from Table 1: (i) the M–N bond distance in metal complexes is adjusted according to the position of the metal atom in the periodic table; (ii) according to the reported data from the literature, the five-membered chelate ring is ideal for lanthanides (4f blocks because of their radii close to 1.0 Å) but experimental data from CSD show that the formation of the five-membered chelate ring is preferred for 4d and 5d metals. To answer this contradiction, we decided to select some complexes based on phen/bpy/en and metal ions with various ranges of radii; Cu^{2+} (r = 0.73 Å), Zn^{2+} (r = 0.74 Å), Cd^{2+} (r = 0.95 Å), Hg^{2+} (r = 1.02 Å), La^{3+} (r = 1.03 Å) and Ba^{2+} (r = 1.35 Å) (see the theoretical part). Moreover, these results clearly confirm, in agreement with previous results,[71] that the model proposed by Hancock[19,69,70] is not adequate to describe these types of complexes. This is due to the fact that it ignores that the angular geometry around the coordination centers is very flexible and it does not take into consideration electronic effects.

8. Theoretical study

We have optimized using DFT calculations (BP86-D3/def2-TZVP, see the ESI† for details) the geometry of several $[ML_3]^{n+}$ complexes where M = Cu, Zn, Cd, Hg, La and Ba and L = phen, bpy and en. The geometric and energetic features of the complexes are gathered in Table 2 and the optimized geometries of the three representative complexes are shown in Fig. S2.† Form the inspection of the results of Table 2 several interesting issues arise. First, the phen complexes are energetically more favorable than the bpy complexes, likely due to the preorganization of the ligand. The en complexes are less favored energetically compared to the phen and bpy ones because the en ligand presents a low preorganization and an intramolecular N–H···N hydrogen bond that is broken upon complexation. Second, the Cu complex is the strongest one in the three series followed by the La complex. The lanthanum complex is more favored than Zn^{2+}, Cd^{2+} and Hg^{2+} complexes likely due to its higher atomic charge (+3 oxidation state). The energetically weakest complex in each series is the Ba^{2+} one that also presents the longest coordination distance (>2.8 Å). The Hg^{2+} complexes exhibit larger chelate ring energies than their corresponding Cd^{2+} complexes, likely due to the lanthanide contraction effect. Third, the average coordination distance (M–N) in Cu is longer than in Zn^{2+} due to the Jahn–Teller effect in the former. Finally,

Table 2 Theoretical calculation of the energy and geometrical parameters of the five-membered chelate rings that are created by phen/bpy/en ligands with M = Cu^{2+}, Zn^{2+}, Cd^{2+}, Hg^{2+}, La^{3+}, Ba^{2+} (ML_3)

	Ionic radius (Å)	Energy of the chelate ring[a] (kcal mol^{-1})	M–N average (Å)	N–N average (Å)	N–M–N average (°)	Ang. 1 average (°)	Ang. 2 average (°)	Ang. 3 average (°)	Ang. 4 average (°)	χ (N–C–C–N) (°)
phen										
Cu	0.73	−311.1	2.253	2.706	77.5	115.3	118.3	117.7	109.7	0.9
Zn	0.74	−287.0	2.192	2.712	76.4	113.5	118.2	118.2	113.5	1.5
Cd	0.95	−234.6	2.376	2.758	70.9	115.3	119.2	119.2	115.3	1.1
Hg	1.02	−259.6	2.427	2.766	69.5	115.8	119.4	119.4	115.8	1.2
La	1.03	−306.7	2.603	2.747	63.7	119.2	118.9	118.9	119.2	1.1
Ba	1.35	−131.9	2.833	2.766	58.4	121.5	119.3	119.3	121.5	0.9
bpy										
Cu	0.73	−296.5	2.156	2.667	76.4	117.4	116.4	115.5	112.5	3.7
Zn	0.74	−274.3	2.187	2.676	75.4	115.7	116.3	116.3	115.7	8.3
Cd	0.95	−221.4	2.371	2.732	70.4	116.7	117.4	117.4	116.7	13.4
Hg	1.02	−246.1	2.421	2.745	69.0	116.9	117.6	117.6	116.9	16.2
La	1.03	−291.8	2.596	2.701	62.7	121.6	116.8	116.8	121.6	8.6
Ba	1.35	−119.8	2.828	2.745	58.1	122.4	117.5	117.5	122.4	17.5
en										
Cu	0.73	−273.6	2.218	2.826	79.1	111.1	109.2	109.1	105.5	55.7
Zn	0.74	−250.8	2.246	2.836	78.4	108.8	109.8	109.8	108.8	56.2
Cd	0.95	−203.4	2.434	2.918	73.7	108.9	110.9	110.9	108.9	60.4
Hg	1.02	−229.1	2.493	2.933	72.1	109.2	111.2	111.2	109.2	61.3
La	1.03	−222.5	2.669	2.924	62.2	116.4	110.4	110.4	116.4	61.6
Ba	1.35	−104.2	2.909	2.999	62.1	111.9	111.5	111.5	111.9	66.2

[a] Computed using the following equation: M(II/III) + L → ML.

the en complexes present longer N–N distances (2.906 Å average) and larger N–C–C–N dihedral angles (60.2°) as expected by the alkyl chain connecting the N-donor atoms.

In general, the trends in the geometric features retrieved from the CSD and those from theoretical calculations are in good agreement. For instance, both experimental and theoretical results indicate that the N–N distances and N–M–N angles are greater for the en ligand complexes and similar for phen and bpy complexes. In addition, the N–M–N angle decreases on going from 3d to 5d transition metals.

9. Inorganic–organic hybrid POMs

As a part of our interest in the preorganized ligands, we have also analyzed polyoxometalates (POMs) as ligands and their participation in the synthesis of inorganic–organic hybrids (IOHs). The motivation comes not only from their intriguing structural diversity but also from their potential applications in many fields such as catalysis,[72–74] magnetic[75] and optical materials and sensitive devices,[76] electro/photochromic systems,[77] sensors[78] and medicine.[79,80] IOH POMs can generally be divided into two categories. Type I comprises the covalent bonds between POMs and MOCs in which POMs, with a large number of terminal and bridging oxygen atoms, act as monodentate or multi-dentate inorganic ligands. The type II category comprises supramolecular assemblies between POMs and MOCs governed by the formation of various non-covalent interactions. Moreover, in the type II category, the POM could simply act as a charge neutralizing agent and/or a void filler.[81] It is noteworthy that many factors influence the final geometry of both categories, which are temperature,[82] pH,[83] nature of the metal ion in the MOCs[84] and the nature of organic ligands.[85,86] Among many types of POMs, Keggin anions with the general formula $\{XM_{12}O_{40}\}^{n-}$ where X is the central atom ($X = B^{3+}$, Si^{4+}, P^{5+}, As^{5+} *etc.*) and M is a metal in a high oxidation state ($M = W^{5+/6+}$, $Mo^{5+/6+}$, $V^{4+/5+}$ *etc.*) have been mostly employed due to their size suitability and structure stability. We have recently demonstrated that Keggin POMs adopt a wide range of coordination numbers (from 1 to 12) in symmetric or asymmetric modes.[81,87]

Although many compounds have been reported based on phen/bpy/en, their IOH POMs are not studied sufficiently yet (see Scheme 2). In this section, we review IOHs constructed using these ligands and Keggin POMs, namely IOH-1/IOH-2/IOH-3 for phen/bpy/en, respectively.

9.1. Synthetic routes of IOHs

Many different preparation methods have been used to synthesize IOHs, which are not easy to crystallize under conventional conditions due to the poor solubility of the organic ligands. The hydro(solvo)thermal (HT) technique, in which high pressure and temperature are used, reduces viscosity and increases ionicity of the solvents. This procedure effectively enhances the solubility of materials and diffusion of the reactants and increases the chances to obtain good-quality crystals. Two strategies have been used for the HT synthesis: (i) *in situ* method, in which POM building blocks are constructed during the reaction and (ii) the use of predefined POMs as building blocks. HT synthesis is the primary method used for the construction of IOHs and there are several parameters that should be considered during the synthesis. These parameters are: the amount of solvent, pH value, temperature, time of the reaction and, in some cases, the order of addition of the reactants to the reaction mixture. Even small deviations from certain synthesis conditions usually result in microcrystalline products, mixtures or amorphous powders.[88]

Some examples of IOH-1–3 synthesized under the HT conditions are shown in Scheme 6 (left), including capped supporting Keggin POMs of formulae $[XM_{12}O_{40}(VO)_a]^{n-}$ where a = 1, 2, 3, which were *in situ* synthesized in the presence of NH_4VO_3, Na_3VO_4, $NaVO_3$ or $VOSO_4$ as auxiliary reactants.[89–91] Mixed-addenda Keggins like $[XM_{12-m}M'_m]^{n-}$ (ref. 92–94) or lacunary Keggins like $[XM_{12-b}O_{40}]^{n-}$ where b = 1, 2, 3, ...[95,96] have also been used for the construction of IOH-1–3 using the *in situ* procedure. In fact, most of the examples reported so far have been synthesized using the *in situ* methodology (Scheme 6 right).

9.2. Features of the hybrid structures

All synthesized IOH-1–3 include transition metals (TMs) as a main part of MOCs (see Fig. S3†). However, no studies have been focused on lanthanides and there are few examples available in the literature. Just recently, Mirzaei *et al.*,[97] Alipour *et al.*[98] and Derakhshanrad *et al.*[99] have reported new hybrids

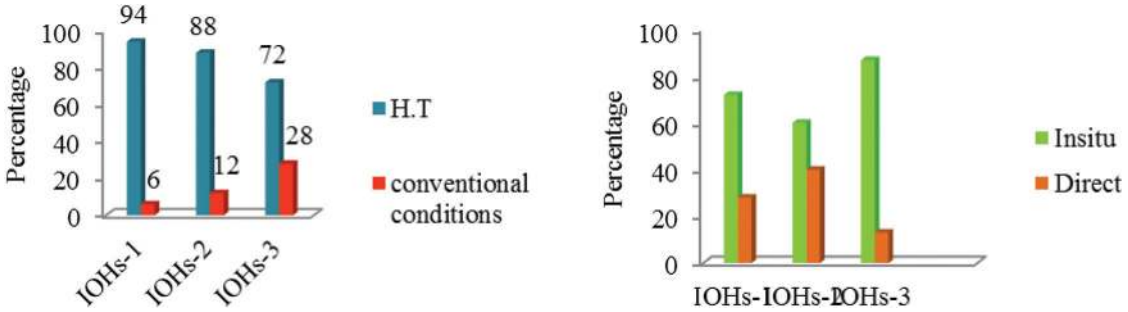

Scheme 6 Left: Percentages of synthetic routes for IOH-1–3. Right: The abundance of two types of HT methods for creating IOH-1–3.

with 1,10-phenanthroline-2,9-dicarboxylic acid and $[SiW_{12}O_{40}]^{4-}$ as ligands and Ce, Nd, Sm and Dy as metal centers. The latter hybrid exhibits ferromagnetic behavior opening up a new window for researchers and crystal engineers for designing POM-based IOHs with new properties taking advantage of the incorporation of the lanthanide.

9.2.1. The nature of organic ligands and the coordination environment around the metal. For the IOH-1–3, the behavior of both types of hybrids (I and II) is summarized in Scheme 7 (left). According to statistics, the probability of finding type I for all three ligands is greater than type II. Furthermore, the reduction of the ligand size from phen to en facilitates the formation of M–O coordination bonds to the Keggin POM ligands. Therefore, the probability of having type I is higher.

The metal coordination environment of the MOCs has been examined and the compounds with auxiliary ligands or having different metals in the structures were not considered. The results show that the majority of IOH-1–3 have [M(phen/bpy/en)], [M(phen/bpy/en)$_2$] or [M(phen/bpy/en)$_3$] stoichiometries. All [M(phen/bpy/en)$_3$] complexes belong to hybrid type II due

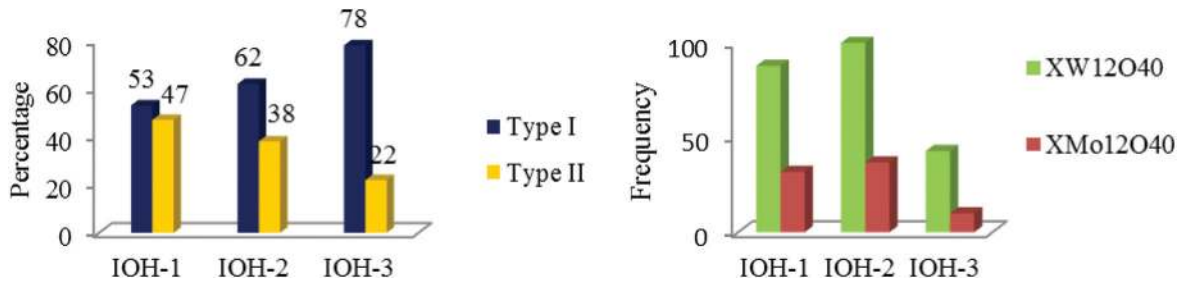

Scheme 7 Left: Percentages of two types of hybrids in the IOH-1–3 and. Right: Categories of IOH-1–3 based on the polyoxomolybdates ($XMo_{12}O_{40}$) and polyoxotungstates ($XW_{12}O_{40}$).

Table 3 Structural and preparation information of IOH-1–3 synthesized by the direct HT method

No.	Formula	Keggin	T (°C)/time (day)	pH	Type	Space group	Ref.
phen							
1	$[Cu(phen)(H_2O)_3]_{0.5}[Cu(phen)_2(H_2O)][PMo_{12}O_{40}]$	$[PMo_{12}O_{40}]^{3-}$	170/6	1.5	II	Triclinic/$P\bar{1}$	114
2	$[Fe(phen)_3]_2[GeMo_{12}O_{40}]\cdot 0.5H_2O$	$[GeW_{12}O_{40}]^{4-}$	175/5	5	II	Triclinic/$P\bar{1}$	115
3	$[Zn(phen)_3]_2[SiW_{12}O_{40}]\cdot 5H_2O$	$[SiW_{12}O_{40}]^{4-}$	160/3	—	II	Triclinic/$P\bar{1}$	116
4	$[Co(phen)_3]_2[SiW_{12}O_{40}]$	$[SiW_{12}O_{40}]^{4-}$	160/3	—	II	Monoclinic/$C2/c$	116
5	$[Ni(phen)_3]_2[SiW_{12}O_{40}]\cdot 2H_2O$	$[SiW_{12}O_{40}]^{4-}$	160/3	—	II	Monoclinic/$C2/c$	116
6	$[Cu(phen)_2]_4[SiW_{12}O_{40}]$	$[SiW_{12}O_{40}]^{4-}$	160/5	—	II	Orthorhombic/$P2_12_12_1$	101
7	$[Fe(phen)_2(H_2O)]_2[PMo_{12}O_{40}]\cdot 2H_2O$	$[PMo_{12}O_{40}]^{3-}$	175/5	5	I	Triclinic/$P\bar{1}$	115
8	$[Zn(phen)_2]_2[PW_{12}O_{40}]$	$[PW_{12}O_{40}]^{3-}$	160/5	2.17	I	Monoclinic/$P2_1/n$	117
9	$K[Zn(phen)_2(H_2O)]_2(OH)[SiW_{12}O_{40}]\cdot H_2O$	$[SiW_{12}O_{40}]^{4-}$	160/5	3.5	I	Triclinic/$P\bar{1}$	117
10	$[Mn(phen)_2(H_2O)]_2[SiW_{12}O_{40}]\cdot nH_2O$	$[SiW_{12}O_{40}]^{4-}$	160/5	2.8	I	Triclinic/$P\bar{1}$	118
11	$[Co(phen)_2(H_2O)]_2[SiW_{12}O_{40}]\cdot nH_2O$	$[SiW_{12}O_{40}]^{4-}$	160/5	3.2	I	Triclinic/$P\bar{1}$	118
12	$[Cu(phen)_2]_2[SiW_{12}O_{40}]$	$[SiW_{12}O_{40}]^{4-}$	160/5	2.8	I	Monoclinic/$P2_1/c$	119
13	$[Cu(phen)(\mu Cl)Cu(phen)_2]_2[SiW_{12}O_{40}]\cdot H_2O$	$[SiW_{12}O_{40}]^{4-}$	160/5	4.2	I	Monoclinic/$P2_1/c$	100
14	$[Cu_2(phen)_4][(GeW_{12}O_{40}]$	$[GeW_{12}O_{40}]^{4-}$	160/4	—	I	Monoclinic/$P2_1/c$	120
15	$\{[Cu(phen)]_3(\mu_2\text{-}Cl)_4\}_2[GeMo_{12}O_{40}]$	$[GeMo_{12}O_{40}]^{4-}$	170/5	4.8	I	Triclinic/$P\bar{1}$	121
bpy							
16	$[Cu(bpy)_2]_2[PMo_{12}O_{40}]\cdot 3H_2O$	$[PMo_{12}O_{40}]^{3-}$	160/10	—	II	Orthorhombic/$Pbca$	122
17	$[Cd(bpy)_3]_2[PMo_{12}O_{40}]$	$[PMo_{12}O_{40}]^{3-}$	160/2	—	II	Monoclinic/$P2_1/c$	123
18	$\{Ag_3(bpy)_6[PW_{12}O_{40}]\}$	$[PW_{12}O_{40}]^{3-}$	160/4	4	II	Monoclinic/$C2/c$	124
19	$[Mn(bipy)_3]_2[SiW_{12}O_{40}]$	$[SiW_{12}O_{40}]^{4-}$	160/5	—	II	Monoclinic/$P2_1/c$	125
20	$[Fe(bpy)_3]_3[H_2W_{12}O_{40}]\cdot 6H_2O$	$[H_2W_{12}O_{40}]^{6-}$	120/2	—	II	Monoclinic/$P2_1/n$	126
21	$[Cu(bpy)_2]_2[HPMo_{12}O_{40}]\cdot 2H_2O$	$[PMo_{12}O_{40}]^{3-}$	160/4	—	I	Orthorhombic/$Pbca$	109
22	$[Cu(bpy)_2](HPMo_{12}O_{40})\cdot H_2O$	$[PMo_{12}O_{40}]^{3-}$	160/3	4.5	I	Orthorhombic/$Pbca$	111
23	$[Cu(bpy)_2](HPW_{12}O_{40})\cdot H_2O$	$[PW_{12}O_{40}]^{3-}$	160/3	4.5	I	Orthorhombic/$Pbca$	111
24	$[Cu(bipy)_2]_2[SiW_{12}O_{40}]$	$[SiW_{12}O_{40}]^{4-}$	160/5	—	I	Orthorhombic/$Pbca$	125
25	$\{[Ni(bpy)_3]_{1.5}[Ni(bpy)_2(H_2O)GeW_{12}O_{40}]\}^-$	$[GeW_{12}O_{40}]^{4-}$	180/3	4.3	I	Monoclinic/$C2/c$	110
26	$[Ni_2(bpy)_4(H_2O)_2(GeW_{12}O_{40})]\cdot 2H_2O$	$[GeW_{12}O_{40}]^{4-}$	160/4	—	I	Monoclinic/$P2_1/c$	120
27	$[Cu(bpy)_2]_2[H_2SiMo_{12}O_{40}]\cdot 2H_2O$	$[SiMo_{12}O_{40}]^{4-}$	160/4	—	I	Orthorhombic/$Pbca$	109
28	$[Ni(bpy)_3]_{1.5}[Ni(bpy)_2(H_2O)BW_{12}O_{40}]$	$[BW_{12}O_{40}]^{5-}$	180/3	4.3	I	Monoclinic/$C2/c$	110
29	$[Co(bpy)_3]_{1.5}\{[Co(bpy)_2(H_2O)][HCoW_{12}O_{40}]\}\cdot 0.5H_2O$	$[HCoW_{12}O_{40}]^{5-}$	160/6	4.3	I	Orthorhombic/$C2/c$	127
30	$[Zn(bpy)_3]_3\{[Zn(bpy)_2(H_2O)]_2[HCoW_{12}O_{40}]_2\}\cdot H_2O$	$[HCoW_{12}O_{40}]^{5-}$	170/4	4–5	I	Orthorhombic/$C2/c$	128
31	$[Zn(bpy)_3]_{1.5}[H_3W_{12}O_{40}Zn(bpy)_2(H_2O)]\cdot 0.5H_2O$	$[H_2W_{12}O_{40}]^{6-}$	120/3	7.5	I	Orthorhombic/$C2/c$	129
32	$[Co(bpy)_3]_3[\{Co(bpy)_2(H_2O)\}_2\{H_3W_{12}O_{40}\}_2]\cdot H_2O$	$[H_2W_{12}O_{40}]^{6-}$	160/5	1.7	I	Monoclinic/$C2/c$	130
33	$[H_2bpy]_{0.5}[\{Cu(bpy)_2\}_2\{H_3W_{12}O_{40}\}]\cdot H_2O$	$[H_2W_{12}O_{40}]^{6-}$	160/5	1.7	I	Monoclinic/$P2_1/n$	130
en							
34	$[Cu(en)_2(H_2O)]_2\{GeW_{12}O_{40}[Cu(en)_2]\}\cdot 2.5H_2O$	$[GeW_{12}O_{40}]^{4-}$	160/10	8.27	I	Monoclinic/$C2/c$	131

to the steric hindrance around the metal ion. On the other hand, the unsaturated [M(phen/bpy/en)] or [M(phen/bpy/en)$_2$] complexes tend to coordinate by the Keggin anions *via* oxygen atoms to complete the metal coordination sphere and both types of hybrids are found.

9.2.2. pH effect. We have analyzed the influence of pH in all IOH-1–3 (see Table 3) synthesized by the direct HT method. We have not considered those where any extra reactant is needed (auxiliary ligands or other metals) or those with capped Keggin POMs in the final structures. According to Table 3, most IOHs with pH < 2 are type II except compounds **2** and **18**. According to Chi *et al.*, the weak coordination ability of POMs increases with increasing pH. Therefore most reactions involving POMs are pH-dependent.[83] As an illustrating case, it is interesting to compare three IOH-3 structures constructed by using only Cu, phen and $SiW_{12}O_{40}$ (SiW) (see Fig. 6). That is, the reaction conditions for **1a**[100] and **1b**[101] were direct HT (with the same reaction temperature and time) and for **1c**[102] was RT, thus **1a** and **1b** are expected to be similar. However, the structural results showed that **1a** and **1c** yield hybrid type I, in sharp contrast to **1b** that yields type II due to the different pH value used for the synthesis. Therefore, the higher the pH, the higher the chance to obtain a hybrid type I is. It is worth mentioning that in **1c**, trilacunary $[SiW_9O_{34}]^{10-}$ is used as a reactant that is transformed into the saturated SiW due to its low stability under the reaction conditions (pH = 6).[102]

9.2.3. The nature of the Keggin POM. Most of the POM-based IOH-1–3 present either polyoxomolybdates ($XMo_{12}O_{40}$) or polyoxotungstates ($XW_{12}O_{40}$) (Scheme 7 right) in the structures, the latter being almost twice more frequent than the former. This may be attributed to the greater stability of heteropolytungstates compared to molybdates, which is due to the lower energy of the d-metal orbitals[103,104] of W. As can be seen in Scheme 8, there is no clear relationship between the charge density of Keggin and its probability of connecting with MOCs to form type I hybrids. Some examples of IOH-1–3 with similar structures synthesized with different Keggin's formula and charge are as follows: (I) Isostructures of IOH-1: $[Cu(Phen)_2]_4[Cu_5Br_4(Phen)_4][XW_{12}O_{40}]\cdot nH_2O$ (X = P, n = 4; X = Al, n = 6; X = B, n = 8),[105] $[Cu(Phen)_2]_4[Cu_5Cl_4(Phen)_4][XW_{12}O_{40}]\cdot nH_2O$ (X = P, n = 4; X = Al, n = 4; X = B, n = 2),[106]

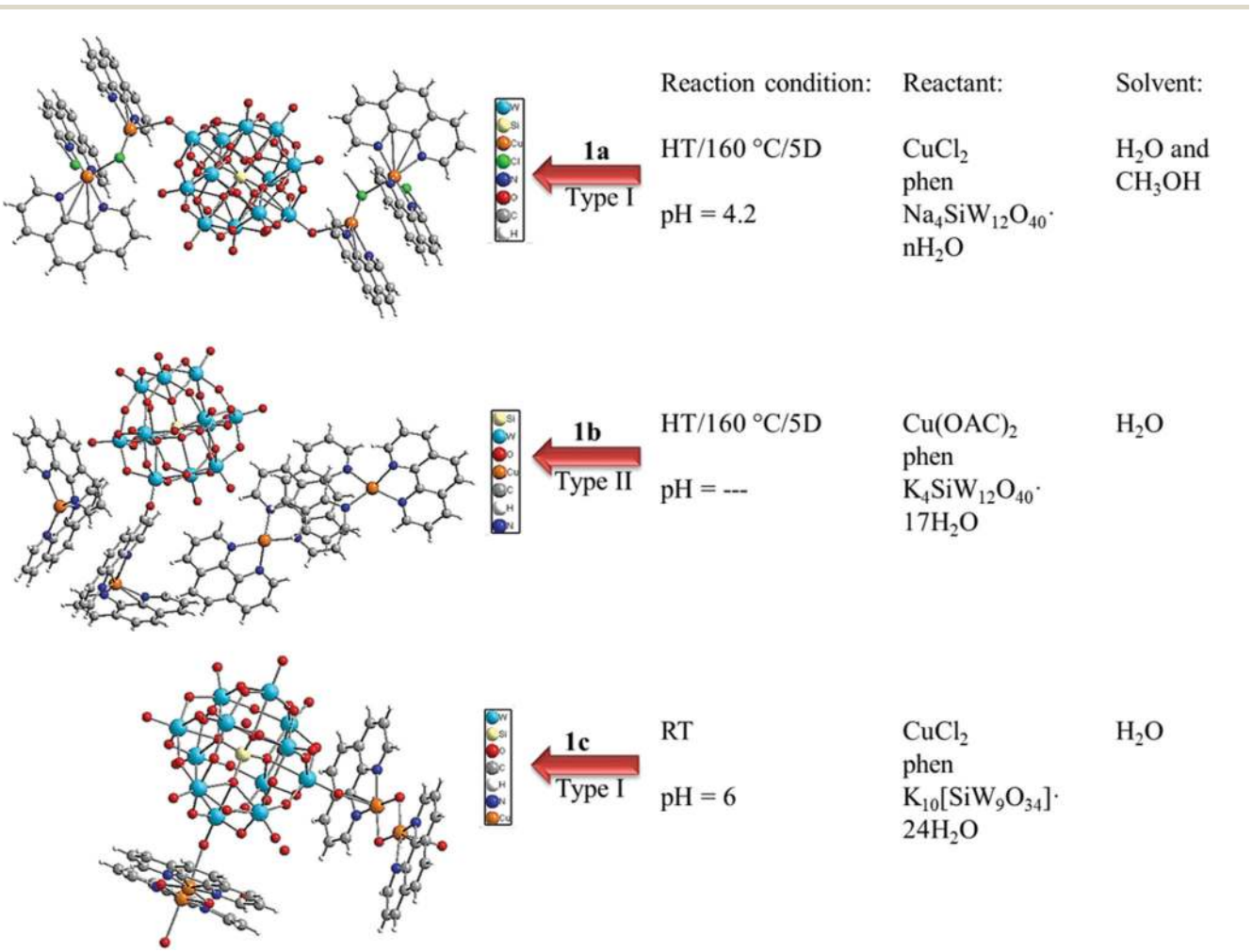

Fig. 6 pH-dependent examples of IOH-1. Figure reproduced from ref. 100–102.

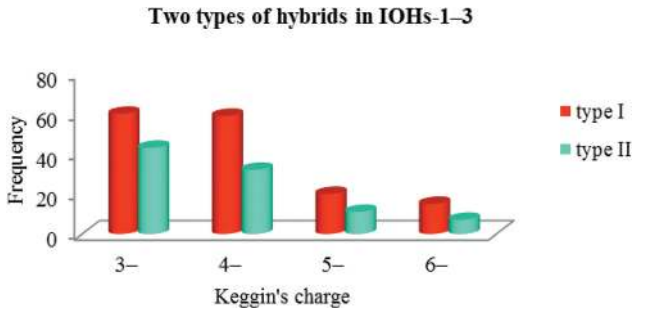

Scheme 8 Numbers of two types of hybrids in IOH-1–3 related to the Keggin's charge.

{[Cu(phen)$_2$]$_2$Cl}[PX$_{12}$O$_{40}$]·H$_2$O (X = Mo and W),[107] [Cu(phen)$_2$]$_4$[XW$_{12}$O$_{40}$] (X = Si, Ge).[101,108] (II) Isostructures of IOH-2: [Cu(bpy)$_2$]$_2$[H$_n$XMo$_{12}$O$_{40}$]·2H$_2$O (X = P, n = 1; X = Si, n = 2),[109] {[Ni(bpy)$_3$]$_{1.5}$[Ni(bpy)$_2$(H$_2$O)XW$_{12}$O$_{40}$]}$^{n-}$ (X = P, n = 0, X = Ge, n = 1; X = B, n = 2),[110] [Cu(bpy)$_2$][(HPX$_{12}$O$_{40}$)]·H$_2$O (X = Mo and W).[111] (III) Isostructures of IOH-3: [Cu(en)$_2$(H$_2$O)]$_3$[XW$_{12}$O$_{40}$] (X = V and Si),[112] [Keggin][Co(en)$_3$]$_3$·6DEF (Keggin = [PW$_{12}$O$_{40}$]$^{3-}$, [PMo$_{12}$O$_{40}$]$^{3-}$, [SiW$_{12}$O$_{40}$]$^{4-}$, DEF = diethylformamide).[113]

Accordingly, it seems that the formula and charge of the Keggin POM do not play a key role in the formation of the supramolecular assemblies. Thus, it is expected that isostructural compounds can be synthesized with different types of Keggin POMs.

10. Conclusion

In this review article we present the less studied aspects of phen/bpy/en ligands. Although several studies have been reported in the literature where these ligands are involved, their full structural and geometrical details have not been analyzed in detail yet from the perspective of preorganization and the ability to form five-membered chelate rings with a wide variety of elements. By means of CSD searches we demonstrate that the distances and angles of the five-membered chelate rings adequately change to fit the requirements of the different metal ions, especially 3d elements. As shown in the theoretical part, the Cu^{2+} (r = 0.74 Å) complexes are energetically more favorable than other elements, especially La^{3+} (r = 1.03 Å and with a higher atomic charge than Cu^{2+}) and Hg^{2+} (r = 1.02 Å) compounds. This result disagrees with the old definition: "five-membered chelate rings promote selectivity for large metal ions with an ionic radius (r^+) close to 1.0 Å",[68,69] and agrees well with some other interpretations derived from experimental and theoretical calculations.[47]

In addition, we provide some interesting facts about their IOH assemblies based on Keggin POMs. In agreement with the above lines, all reported IOH-1–3 include TMs as a main part of MOCs (not large metal ions like Lns). We have also summarized some key geometric and synthetic features that favored the formation of IOHs belonging to either type I or II.

Conflicts of interest

The authors declare no conflict of interest.

Acknowledgements

MM would like to thank the financial support by the Ferdowsi University of Mashhad, Mashhad, Iran (grant no. 3/42202). The authors gratefully acknowledge the Cambridge Crystallographic Data Centre (CCDC) for access to the Cambridge Structural Database. AF and AF thank the MINECO/AEI (project CTQ2017-85821-R, FEDER funds) for financial support. A. Franconetti thanks MINECO/AEI from SPAIN for a "Juan de la Cierva" contract.

References

1 C. B. Aakeröy, N. R. Champness and C. Janiak, *CrystEngComm*, 2010, **12**, 22–43.
2 T. S. Thakur, R. Dubey and G. R. Desiraju, *Annu. Rev. Phys. Chem.*, 2015, **66**, 21–42.
3 D. Braga, F. Grepioni, L. Maini and S. D'Agostino, *IUCrJ*, 2017, **4**, 369–379.
4 G. R. Desiraju, *J. Mol. Struct.*, 2003, **656**, 5–15.
5 J. R. Lundgren and M. Stradiotto, *Ligand Design in Metal Chemistry*, John Wiley & Sons, Ltd, Chichester, UK, 2016.
6 F. C. Pigge, *CrystEngComm*, 2011, **13**, 1733–1748.
7 M. D. Fryzuk, *Inorg. Chem.*, 2015, **54**, 9671–9674.
8 B. P. Hay and R. D. Hancock, *Coord. Chem. Rev.*, 2001, **212**, 61–78.
9 J. M. Lehn, *Eur. Rev.*, 2009, **17**, 263–280.
10 P. Comba and W. Schiek, *Coord. Chem. Rev.*, 2003, **239**, 21–29.
11 S. Taleghani, M. Mirzaei, H. Eshtiagh-hosseini and A. Frontera, *Coord. Chem. Rev.*, 2016, **309**, 84–106.
12 F. Taghipour and M. Mirzaei, *Acta Crystallogr., Sect. C: Struct. Chem.*, 2019, **75**, 231–247.
13 J.-P. Zeng, H. Cong, K. Chen, S.-F. Xue, Y.-Q. Zhang, Q.-J. Zhu, J.-X. Liu and Z. Tao, *Inorg. Chem.*, 2011, **50**, 6521–6525.
14 S. Wang, F. Hu, J. Zhou, Y. Zhou, Q. Huang and J. Lang, *Cryst. Growth Des.*, 2015, **15**, 4087–4097.
15 C. Huang, A. Parish, F. Samain, F. Garo, R. Ha and J. R. Morrow, *Bioconjugate Chem.*, 2010, **21**, 476–482.
16 F. Li, G. Zhao, H. Wu, H. Lin and X. Wu, *J. Inorg. Biochem.*, 2006, **100**, 36–43.
17 F. E. Poynton, S. A. Bright, S. Blasco, D. C. Williams, J. M. Kelly and T. Gunnlaugsson, *Chem. Soc. Rev.*, 2017, **46**, 7706–7756.
18 N. Leygue, A. Boulay, C. Galaup, E. Benoist, S. Laurent, L. Vander Elst, B. Mestre-Voegtlé and C. Picard, *Dalton Trans.*, 2016, **45**, 8379–8393.
19 D. L. Melton, D. G. VanDerveer and R. D. Hancock, *Inorg. Chem.*, 2006, **45**, 9306–9314.

20 Z. D. Liu and R. C. Hider, *Coord. Chem. Rev.*, 2002, **232**, 151–171.
21 M. J. Sever, J. T. Weisser, J. Monahan, S. Srinivasan and J. J. Wilker, *Angew. Chem., Int. Ed.*, 2004, **43**, 448–450.
22 R. D. Hancock, *Chem. Soc. Rev.*, 2013, **42**, 1500–1524.
23 G. Accorsi, A. Listorti, K. Yoosaf and N. Armaroli, *Chem. Soc. Rev.*, 2009, **38**, 1690.
24 G. Ma, A. Fischer, R. Nieuwendaal, K. Ramaswamy and S. E. Hayes, *Inorg. Chim. Acta*, 2005, **358**, 3165–3173.
25 W.-S. Han, J. Han, H. Kim, M. J. Choi, Y.-S. Kang, C. Pac and S. O. Kang, *Inorg. Chem.*, 2011, **50**, 3271–3280.
26 I. V. Solovyev, A. Kondinski, K. Y. Monakhov, I. O. Koshevoy and E. V. Grachova, *Inorg. Chem. Front.*, 2018, **5**, 160–171.
27 K. O. Kirlikovali, J. C. Axtell, A. Gonzalez, A. C. Phung, S. I. Khan and A. M. Spokoyny, *Chem. Sci.*, 2016, **7**, 5132–5138.
28 R. T. F. Jukes and B. Bozic, *ChemPhysChem*, 2006, **45**, 177–185.
29 B. Higgins, B. A. DeGraff and J. N. Demas, *Inorg. Chem.*, 2005, **44**, 6662–6669.
30 I. Bist, B. Song, I. M. Mosa, T. E. Keyes, A. Martin, R. J. Forster and J. F. Rusling, *ACS Sens.*, 2016, **1**, 272–278.
31 L. Yang, X. Li, X. Li, S. Yan, Y. Ren, M. Wang, P. Liu, Y. Dong and C. Zhang, *Anal. Biochem.*, 2016, **492**, 56–62.
32 P. Gayathri and A. Senthil Kumar, *Langmuir*, 2014, **30**, 10513–10521.
33 A. Kim, S. Ryu and H. Jung, *Adv. Mater. Interfaces*, 2016, **3**, 1500449.
34 G. Lemercier, M. Four and S. Chevreux, *Coord. Chem. Rev.*, 2018, **368**, 1–12.
35 T. Ohshita, A. Tsukamoto and M. Senna, *Phys. Status Solidi*, 2004, **201**, 762–768.
36 S. C. Marker, S. N. MacMillan, W. R. Zipfel, Z. Li, P. C. Ford and J. J. Wilson, *Inorg. Chem.*, 2018, **57**, 1311–1331.
37 D. W. Thompson, A. Ito and T. J. Meyer, *Pure Appl. Chem.*, 2013, **85**, 1257–1305.
38 T. A. White, S. L. H. Higgins, S. M. Arachchige and K. J. Brewer, *Angew. Chem., Int. Ed.*, 2011, **50**, 12209–12213.
39 D. V. Scaltrito, D. W. Thompson, J. A. O'Callaghan and G. J. Meyer, *Coord. Chem. Rev.*, 2000, **208**, 243–266.
40 D. J. Cram, *Angew. Chem., Int. Ed. Engl.*, 1988, **27**, 1009–1020.
41 V. Martí-Centelles, M. D. Pandey, M. I. Burguete and S. V. Luis, *Chem. Rev.*, 2015, **115**, 8736–8834.
42 E. Lee, S. Young, L. F. Lindoy and S. Sung, *Coord. Chem. Rev.*, 2013, **257**, 3125–3138.
43 L. F. Lindoy, K. Park and S. S. Lee, *Chem. Soc. Rev.*, 2013, **42**, 1713–1727.
44 A. Najafi, M. Mirzaei and J. T. Mague, *CrystEngComm*, 2016, **18**, 6724–6737.
45 A. N. Carolan, G. M. Cockrell, N. J. Williams, G. Zhang, D. G. VanDerveer, H. Lee, R. P. Thummel and R. D. Hancock, *Inorg. Chem.*, 2013, **52**, 15–27.
46 L. Yalçin and R. Öztürk, *J. Optoelectron. Adv. Mater.*, 2013, **15**, 326–334.
47 X.-J. Sun, Y.-F. Cheng, J. Feng and X.-M. Lu, *J. Chin. Chem. Soc.*, 2013, **60**, 511–515.
48 K. A. McGee and K. R. Mann, *J. Am. Chem. Soc.*, 2009, **131**, 1896–1902.
49 J. M. Harrowfield, Y. Kim, B. W. Skelton, A. N. Sobolev and A. H. White, *CrystEngComm*, 2017, **19**, 2372–2379.
50 A. Naim, Y. Bouhadja, M. Cortijo, E. Duverger-Nédellec, H. D. Flack, E. Freysz, P. Guionneau, A. Iazzolino, A. Ould Hamouda, P. Rosa, O. Stefańczyk, Á. Valentín-Pérez and M. Zeggar, *Inorg. Chem.*, 2018, **57**, 14501–14512.
51 T. Sakai, Z. Taira, S. Yamazaki and T. Ama, *Polyhedron*, 1989, **8**, 1989–1993.
52 G. Bombieri, G. Bruno, M. D. Grillone and G. Polizzotti, *Acta Crystallogr., Sect. C: Cryst. Struct. Commun.*, 1984, **40**, 2011–2014.
53 J. H. N. Buttery, Effendy, S. Mutrofin, N. C. Plackett, B. W. Skelton, N. Somers, C. R. Whitaker and A. H. White, *Z. Anorg. Allg. Chem.*, 2006, **632**, 1839–1850.
54 R. Giri and J. F. Hartwig, *J. Am. Chem. Soc.*, 2010, **132**, 15860–15863.
55 V. Lingen, A. Lüning, C. Straußß, I. Pantenburg, G. B. Deacon, A. Klein and G. Meyer, *Eur. J. Inorg. Chem.*, 2013, **2013**, 4450–4458.
56 D. M. Tsymbarenko, I. E. Korsakov, K. A. Lyssenko and S. I. Troyanov, *Polyhedron*, 2015, **92**, 68–76.
57 B. W. Skelton, A. F. Waters and A. H. White, *Aust. J. Chem.*, 1996, **49**, 99–115.
58 X. Tai, J. Yin and M. Hao, *Acta Crystallogr., Sect. E: Struct. Rep. Online*, 2007, **63**, m1827–m1827.
59 L. Engelhardt, D. Kepert, J. Patrick and A. White, *Aust. J. Chem.*, 1989, **42**, 329–334.
60 A. H. Göller and U. Grummt, *Chem. Phys. Lett.*, 2002, **354**, 233–242.
61 B. Butschke and H. Schwarz, *Organometallics*, 2010, **29**, 6002–6011.
62 I. L. Fedushkin, T. V. Petrovskaya, F. Girgsdies, V. I. Nevodchikov, R. Weimann, H. Schumann and M. N. Bochkarev, *Russ. Chem. Bull.*, 2000, **49**, 1869–1876.
63 S. Fortier, J. Veleta, A. Pialat, J. Le Roy, K. B. Ghiassi, M. M. Olmstead, A. Metta-Magaña, M. Murugesu and D. Villagrán, *Chem. – Eur. J.*, 2016, **22**, 1931–1936.
64 M. Kadarkaraisamy, D. P. Engelhart, P. N. Basa and A. G. Sykes, *J. Coord. Chem.*, 2010, **63**, 2261–2267.
65 H. T. Sartain, R. J. Staples and S. M. Biros, *Acta Crystallographica, Section E: Structure Reports Online*, 2014, **70**, 424–426.
66 S. R. Maqsood, N. Islam, S. Bashir, B. Khan and A. H. Pandith, *J. Coord. Chem.*, 2013, **66**, 2308–2315.
67 A. Bencini and V. Lippolis, *Coord. Chem. Rev.*, 2010, **254**, 2096–2180.
68 R. D. Hancock, *J. Chem. Educ.*, 1992, **69**, 615.
69 R. D. Hancock, D. L. Melton, J. M. Harrington, F. C. McDonald, R. T. Gephart, L. L. Boone, S. B. Jones,

N. E. Dean, J. R. Whitehead and G. M. Cockrell, *Coord. Chem. Rev.*, 2007, **251**, 1678–1689.
70 N. E. Dean, R. D. Hancock, C. L. Cahill and M. Frisch, *Inorg. Chem.*, 2008, **47**, 2000–2010.
71 P. Comba and M. Kerscher, *Coord. Chem. Rev.*, 2009, **253**, 564–574.
72 M. A. Fashapoyeh, M. Mirzaei, H. Eshtiagh-hosseini, A. Rajagopal, M. Lechner, R. Liu and C. Streb, *Chem. Commun.*, 2018, **54**, 10427–10430.
73 M. M. Heravi, M. Mirzaei, S. Y. S. Beheshtiha, V. Zadsirjan, F. Mashayekh Ameli and M. Bazargan, *Appl. Organomet. Chem.*, 2018, **32**, e4479.
74 J. Ettedgui, Y. Diskin-Posner, L. Weiner and R. Neumann, *J. Am. Chem. Soc.*, 2011, **133**, 188–190.
75 J. M. Clemente-Juan, E. Coronado and A. Gaita-Ariño, *Chem. Soc. Rev.*, 2012, **41**, 7464–7478.
76 E. Coronado, C. Giménez-Saiz and C. J. Gómez-García, *Coord. Chem. Rev.*, 2005, **249**, 1776–1796.
77 J. J. Walsh, A. M. Bond, R. J. Forster and T. E. Keyes, *Coord. Chem. Rev.*, 2016, **306**, 217–234.
78 C. Zhou, S. Li, W. Zhu, H. Pang and H. Ma, *Electrochim. Acta*, 2013, **113**, 454–463.
79 M. Arefian, M. Mirzaei, H. Eshtiagh-Hosseini and A. Frontera, *Dalton Trans.*, 2017, **46**, 6812–6829.
80 A. Sakamoto, K. Unoura and H. Nabika, *J. Phys. Chem. C*, 2018, **122**, 1404–1411.
81 M. Mirzaei, H. Eshtiagh-hosseini, M. Alipour and A. Frontera, *Coord. Chem. Rev.*, 2014, **275**, 1–18.
82 G. Hou, L. Bi, B. Li and L. Wu, *Inorg. Chem.*, 2010, **49**, 6474–6483.
83 Y. N. Chi, F. Y. Cui, A. R. Jia, X. Y. Ma and C. W. Hu, *CrystEngComm*, 2012, **14**, 3183–3188.
84 J. Sosa, T. Bennett, K. Nelms, B. Liu, R. Tovar and Y. Liu, *Crystals*, 2018, **8**, 325.
85 Y. P. Ren, X. J. Kong, X. Y. Hu, M. Sun, L. S. Long, R. Bin Huang and L. S. Zheng, *Inorg. Chem.*, 2006, **45**, 4016–4023.
86 P. P. Zhang, J. Peng, J. Q. Sha, A. X. Tian, H. J. Pang, Y. Chen and M. Zhu, *CrystEngComm*, 2009, **11**, 902–908.
87 M. Mirzaei, H. Eshtiagh-hosseini, M. Alipour, A. Bauzá, J. T. Mague, M. Korabik and A. Frontera, *Dalton Trans.*, 2015, **44**, 8824–8832.
88 X. M. Zhang, *Coord. Chem. Rev.*, 2005, **249**, 1201–1219.
89 L. Dai, Y. Ma, E. Wang, Y. Lu, X. Xu and X. Bai, *Transition Met. Chem.*, 2006, **31**, 340–346.
90 J.-W. Cui, X. Cui, H. Yu, J. Xu, Z. Yi and W. Duan, *Inorg. Chim. Acta*, 2008, **361**, 2641–2647.
91 L.-M. Wang, Y. Wang, Y. Fan, L. Xiao, Y. Hu, Z. Gao, D.-F. Zheng, X. Cui and J. Xu, *CrystEngComm*, 2014, **16**, 430–440.
92 C. Li, R. Cao, K. P. O'Halloran, H. Ma and L. Wu, *Electrochim. Acta*, 2008, **54**, 484–489.
93 H. Liu, Y. Sun, Y.-G. Chen, F.-X. Meng and D.-M. Shi, *J. Coord. Chem.*, 2008, **61**, 3102–3109.
94 L. Dai, W. You, E. Wang, S. Wu, Z. Su, Q. Du, Y. Zhao and Y. Fang, *Cryst. Growth Des.*, 2009, **9**, 2110–2116.
95 J. Song, Z. Luo, H. Zhu, Z. Huang, T. Lian, A. L. Kaledin, D. G. Musaev, S. Lense, K. I. Hardcastle and C. L. Hill, *Inorg. Chim. Acta*, 2010, **363**, 4381–4386.
96 C. Pichon, A. Dolbecq, P. Mialane, J. Marrot, E. Rivière, M. Goral, M. Zynek, T. McCormac, S. A. Borshch, E. Zueva and F. Sécheresse, *Chem. – Eur. J.*, 2008, **14**, 3189–3199.
97 M. Mirzaei, H. Eshtiagh-Hosseini and A. Hassanpoor, *Inorg. Chim. Acta*, 2019, **484**, 332–337.
98 M. Alipour, O. Akintola, A. Buchholz, M. Mirzaei, H. Eshtiagh-Hosseini, H. Görls and W. Plass, *Eur. J. Inorg. Chem.*, 2016, **2016**, 5356–5365.
99 S. Derakhshanrad, M. Mirzaei, A. Najafi, C. Ritchie, A. Bauzá, A. Frontera and J. T. Mague, *Acta Crystallogr., Sect. C: Struct. Chem.*, 2018, **74**, 1300–1309.
100 Q. X. Han, Y. M. Cheng, J. Li and J. P. Wang, *Russ. J. Coord. Chem.*, 2011, **37**, 547–551.
101 Y. Wang, D. Xiao, E. Wang, L. Fan and J. Liu, *Transition Met. Chem.*, 2007, **32**, 950–959.
102 T. Wang, J. Peng, H. Liu, D. Zhu, A. Tian and L. Wang, *J. Mol. Struct.*, 2008, **892**, 268–271.
103 J. M. Maestre, X. Lopez, C. Bo, J. Poblet and N. Casañ-Pastor, *J. Am. Chem. Soc.*, 2001, **123**, 3749–3758.
104 J. M. Poblet, X. López and C. Bo, *Chem. Soc. Rev.*, 2003, **32**, 297–308.
105 L. Xiao, Y. Hu, L.-M. Wang, Y. Wang, J. Xu, H. Ding, X. Cui and J.-Q. Xu, *CrystEngComm*, 2012, **14**, 8589–8596.
106 L.-N. Xiao, Y. Wang, C.-L. Pan, J.-N. Xu, T.-G. Wang, H. Ding, Z.-M. Gao, D.-F. Zheng, X.-B. Cui and J.-Q. Xu, *CrystEngComm*, 2011, **13**, 4878.
107 X. Lu, X. Shi, Y. Bi, C. Yu, Y. Chen and Z. Chi, *Eur. J. Inorg. Chem.*, 2009, **2009**, 5267–5276.
108 Y. Hu, L. Xiao, Y. Wang, D. Zhao, L. Wang, H. Guo, X. Cui and J. Xu, *Polyhedron*, 2013, **56**, 152–159.
109 J. Chen, J. Sha, J. Peng, Z. Shi, B. Dong and A. Tian, *J. Mol. Struct.*, 2007, **846**, 128–133.
110 C.-J. Wang, S. Yao, Y.-Z. Chen, Z.-M. Zhang and E.-B. Wang, *RSC Adv.*, 2016, **6**, 99010–99015.
111 T. Li, J. Lü, S. Gao and R. Cao, *Inorg. Chem. Commun.*, 2007, **10**, 551–554.
112 Y. Lu, X. Cui, Y. Chen, J. Xu, Q. Zhang, Y. Liu, J.-Q. Xu and T. Wang, *J. Solid State Chem.*, 2009, **182**, 2111–2117.
113 C. Dey, R. Das, P. Pachfule, P. Poddar and R. Banerjee, *Cryst. Growth Des.*, 2011, **11**, 139–146.
114 Z. Han, Y. Wang, J. Wu and X. Zhai, *Solid State Sci.*, 2011, **13**, 1560–1566.
115 J. Sha, J. Peng, H. Liu, J. Chen, A. Tian, B. Dong and P. Zhang, *J. Coord. Chem.*, 2008, **61**, 1221–1233.
116 R.-d. H. Y.-f. Zhang, Y.-y. Jia, H.-l. Nie, X.-j. Yan and L. Wang, *Chem. Res. Chin. Univ.*, 2010, **26**, 683–686.
117 K. Alimaje, X. Wang, Z. Zhang, J. Peng, Z. Shi, X. Yu and Z. Ren, *J. Cluster Sci.*, 2013, **24**, 1021–1030.
118 S. Lu, F.-X. Meng, D.-M. Shi and Y. Chen, *Transition Met. Chem.*, 2008, **33**, 353–359.
119 F. Meng, J. Sun, K. Liu, F. Ma and Y. Chen, *J. Coord. Chem.*, 2007, **60**, 401–410.

120 B. Zhang, C. Wu, J. Qiu, Y. Li and Z. Liu, *J. Coord. Chem.*, 2014, **67**, 787–796.
121 S. Li, P. Ma, H. Niu, J. Zhao and J. Niu, *Inorg. Chem. Commun.*, 2010, **13**, 805–808.
122 C. Liu, J.-Y. Zhang and D. Zhang, *J. Coord. Chem.*, 2008, **61**, 627–639.
123 T.-Y. Lan, J.-X. Chen, X.-Q. Lü, Y.-B. Huang, Z.-S. Li, C.-X. Wei and Z.-C. Zhang, *Struct. Chem.*, 2006, **17**, 35–41.
124 X. Lu, Y. Luo, C. Lu, X. Chen and H. Zhang, *J. Solid State Chem.*, 2015, **232**, 123–130.
125 R. Chatterjee, M. Ali, M. G. B. Drew, M. Nethaji, S. Mondal and M. Mukherjee, *Transition Met. Chem.*, 2009, **34**, 1–5.
126 Y. Li, D. G. Hubble, R. G. Miller, H. Zhao, W. Pan, S. Parkin and B. Yan, *Polyhedron*, 2010, **29**, 3324–3328.
127 J. Sha, J. Peng, J. Chen, H. Liu, A. Tian and P. Zhang, *Solid State Sci.*, 2007, **9**, 1012–1019.
128 H. WANG, C. CHENG and Y. TIAN, *Chinese J. Chem.*, 2009, **27**, 1099–1102.
129 B. Yan, Y. Li, H. Zhao, W. Pan and S. Parkin, *Inorg. Chem. Commun.*, 2009, **12**, 1139–1141.
130 C. Zhang, H. Pang, D. Wang and Y.-G. Chen, *J. Coord. Chem.*, 2010, **63**, 568–578.
131 J. Wang, Y. Feng, P. Ma and J. Niu, *J. Coord. Chem.*, 2009, **62**, 1895–1901.